

High Energy Neutron Time of Flight Measurements of Carbon and Beryllium Samples at the RPI LINAC

M. Rapp, Y. Danon, R. C. Block, F. Saglime, R. Bahran
Rensselaer Polytechnic Institute
Department of Mechanical, Aerospace, and Nuclear Engineering
Troy, New York 12180-3590

G. Leinweber, D. P. Barry, N. J. Drindak (ret), J. G. Hoole
Knolls Atomic Power Laboratory
P.O. Box 1072, Schenectady, New York 12301-1072

ABSTRACT

New high energy (0.5-20 MeV) beryllium total cross sections have been measured at the Gaertner Linac Laboratory located at Rensselaer Polytechnic Institute. The transmission measurement combines fast detector response and electronics, a narrow neutron pulse width and 100 meter flight path. The detector system was validated using the well known cross sections of carbon. An innovative background determination technique was developed and applied. Cross sections derived from both the carbon and beryllium data are compared to ENDF/B-VII.0. This effort validates the newly developed 100 meter time of flight system and data analysis methods and provides useful information to improve the current data for beryllium.

Key Words: Beryllium, Cross Section, Transmission, Time of Flight

1. INTRODUCTION

1.1. Detector Design

Measurements were done at the Gaertner Laboratory 100 meter flight station utilizing the RPI modular proton recoil detector. This detector consists of two Eljen Technology Model 510-50X70X138/301 EJ-301 liquid scintillator modules [1]. Each module is 5.0 inches thick, 7.2 inches wide and 14.0 inches long, with two photomultiplier tubes to optimize light collection throughout the detector volume. The two modules stacked on top of each other give a total front face area to the detector system of 14.4 inches high by 14.0 inches wide. This area was established to optimize collection of the neutron beam profile at the detector location, which was determined through calculation using the Monte Carlo transport code MCNP5 [2] and verified with experimental data. The thickness of the detector was selected to maximize efficiency while maintaining good time resolution.

1.2. System Electronics

The detector system was designed with fast electronics to take advantage of the five-nanosecond wide neutron pulse being generated by the RPI linear accelerator. Figure 1 shows the electronics and signal path used in the system. Events detected in each module are fed to an ORTEC 935 constant fraction discriminator for optimizing time resolution over the wide range of pulse amplitudes and then summed in an ORTEC CO4020 logic unit. This output is then converted to an optical signal for transport to the data acquisition computer using a LuxLink DX7201 Fiber Optic TTL Transmission System. The data acquisition computer houses a FAST ComTec P7889 Time of Flight Multiscaler board with one picosecond time resolution. The narrow (5-10 nsec) neutron pulse width along with the 100 meter flight path allows for high resolution time of flight data to be collected, necessary for measurements in this energy range.

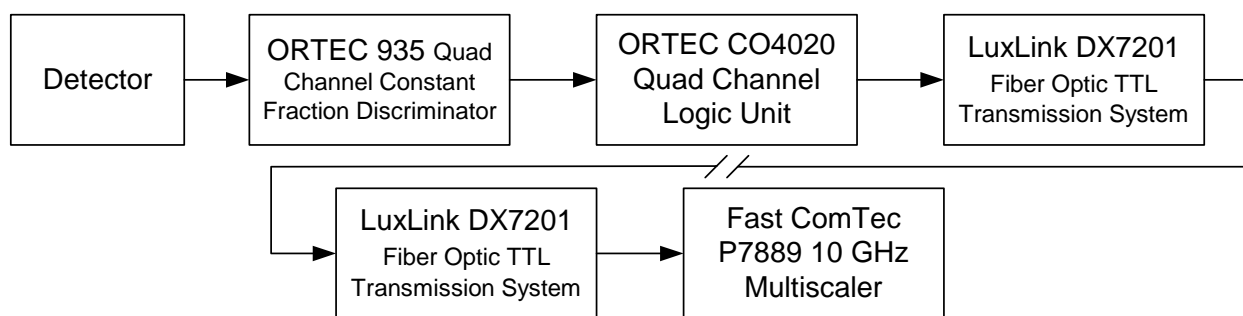


Figure 1: Block diagram of data acquisition electronics

2. DATA COLLECTION

2.1. Neutron Production

Neutrons are produced at the Gaertner Lab via a pulsed electron beam from the linear accelerator striking the water cooled tantalum plates in the RPI neutron producing target [3]. The high energy electrons from the linear accelerator generate bremsstrahlung x-rays within the target which interact with the tantalum to produce photoneutrons. These neutrons are then collimated within the center drift tube of the time of flight facility to ensure no neutrons can stream around the sample material and reach the detector. The RPI target was placed on axis with the flight tube and used without a moderator to enhance neutron production in the high energy of interest. The repetition rate was 400 pulses per second with a pulse width of 5.2 nsec; average current on target was 3.5 μ A with electron energy of 54 MeV.

2.2. Collection Method

The time of flight method was used to determine the energy of the neutrons interacting with the detector. The flight path distance from target to detector was determined to be 99.95 ± 0.07 meters by fitting experimental data to the well known carbon cross sections. The zero time of flight was determined from the gamma flash, visible in the data, which occurs near simultaneous

with the production of neutrons in the target. This time was corrected for the photon flight time and used to determine the energy of each neutron time of flight bin.

Data were collected for 3 beryllium samples (2 cm, 4 cm and 8 cm thick) and 1 carbon sample (13 cm thick). Both the beryllium and carbon samples were analyzed to be greater than 99.9% pure. Multiple beryllium samples were used to optimize the sample counting statistics while minimizing the total run time [4]. Using multiple samples also allows for the comparison of the individual sample cross section data prior to combining as a means of verification.

The process of placing and removing the samples relative to the beam is accomplished by a computer controlled sample changer wheel, to which the samples are mounted. The sample changer ensures that each sample is positioned in the centerline of the flight path and allows for repeatable data cycles. Short data cycles (i.e. the time each sample is in the beam for each full rotation of the sample changer wheel) are used to reduce the effect of data fluctuations due to changing beam characteristics. Additionally, neutron monitors are used to measure the relative intensity of neutron production over the data cycles.

3. DATA ANALYSIS

3.1. Transmission Calculation

Transmission in each time bin is the ratio of the counting rate with the sample in the beam divided by open beam, as given by equation 1. The neutron monitor data is used as a normalization factor to account for variation in neutron beam intensity during data taking.

$$T_i = \left[\frac{C_i^S - B_i^S}{C_i^O - B_i^O} \right] \frac{mon^O}{mon^S} \quad (1)$$

Where: T_i is the transmission in the time of flight channel i

C_i^S is the dead time corrected counting rate of the sample measurement

B_i^S is the background counting rate of the sample measurement

C_i^O is the dead time corrected counting rate of the open beam measurement

B_i^O is the background counting rate of the open beam measurement

mon^O is the monitor counts for the open beam measurement

mon^S is the monitor counts for the sample measurement

3.2. Background Determination Method

Two components contribute to the background counting rates given in equation 1. The first is the room background, which is time independent. The second component is associated with the production and transport of the pulsed neutron beam and varies with time. The room background can be easily obtained by collecting data with the Linac off. The time dependent background can only be obtained during operation and is therefore masked by the neutron spectrum.

It was observed in the data that a component of background built up over time and then exponentially decays to room background at long time of flight. Neutrons moderated in the detector followed by the thermal capture in hydrogen were suspected due to the exponential decay seen in the data. MCNP simulations were used to investigate this source of background. It was determined that this component is due to 2.2 MeV photons from the hydrogen capture of the neutrons in the liquid scintillator material. This was demonstrated by comparing the rate of decay from the simulation to the experimental data.

A method was developed which uses MCNP5 to model the gammas released from neutron capture within the detector. The problem involves the transport of a spectrum of neutrons, modeled to be very similar to that observed at the RPI LINAC, through samples of equal dimensions to those of the experiment into a simulated detector volume. The resulting photon tally, shown in Figure 2, is a combination of both 2.2 MeV photons from neutron capture and 4.4 MeV photons from inelastic scattering of the incident neutrons in the EJ-301 liquid.

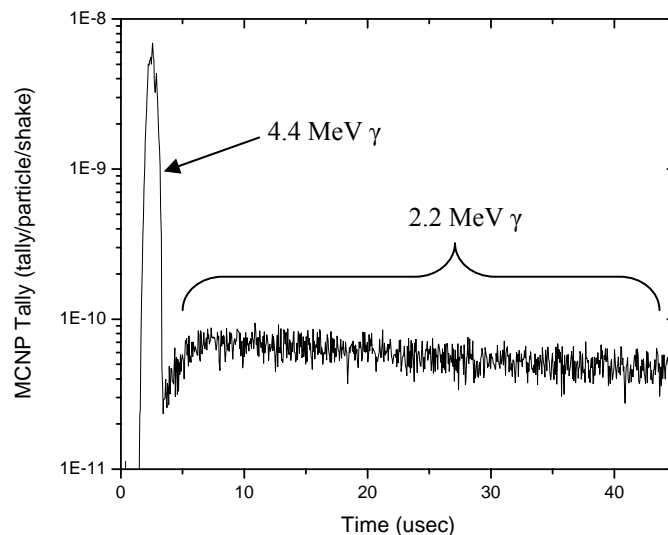


Figure 2: MCNP calculation showing combination of 4.4 MeV inelastic scattering photons and 2.2 MeV capture resulting from neutron interaction with EJ-301 liquid

This tally is then normalized to fit the tail in time of the experimental data, after primary neutrons from the target have passed. The 4.4 MeV inelastic scattering photons do not contribute to the background since they are emitted instantaneously and therefore provide indication of a primary neutron interaction. This effect is therefore neglected in the calculation of time dependent background and the 2.2 MeV curve is extrapolated to the room background as seen in Figure 3.

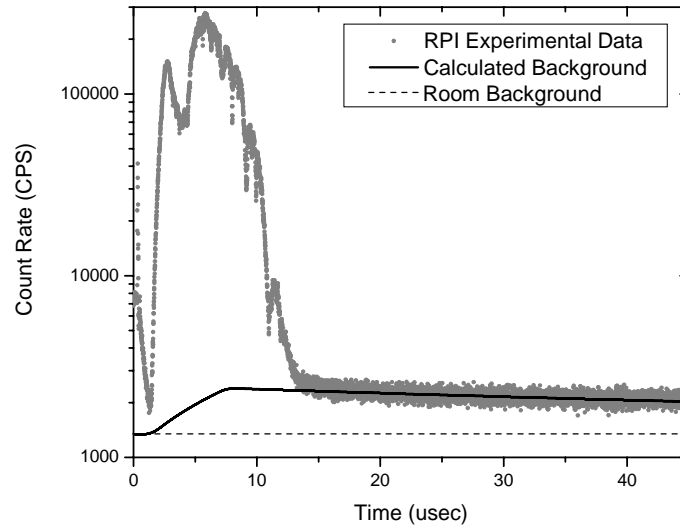


Figure 3: Fitted 2.2 MeV photon background overlaid on 2 cm beryllium experimental data

3.3. Cross Section Calculation

From the calculated transmission the cross section at time of flight channel i can be determined using equation 2.

$$\sigma_i = -\frac{1}{N} \ln(T_i) \quad (2)$$

Where: σ_i is the total cross section in barns in the time of flight channel i

T_i is the transmission in the time of flight channel i

N is the atomic number density of the sample in atoms/barn

The atomic number density of the samples must first be determined. These were calculated for each sample using equation 3; sample diameter and mass values are shown in Table I.

$$N = \frac{mN_A}{A\pi\left(\frac{D}{2}\right)^2} \quad (3)$$

Where: m is the sample mass

N_A is Avogadro's number

A is the sample atomic mass

D is the sample diameter

Table I: Sample measurements

Sample	Thickness (cm)	Diameter (cm)	Mass (g)	Number Density (atoms/b)
beryllium	2	7.498±0.003	163.08±0.01	0.24684±0.00008
beryllium	4	7.503±0.003	326.61±0.01	0.49369±0.00016
beryllium	8	7.501±0.003	653.06±0.01	0.98795±0.00033
carbon	13	7.498±0.003	968.80±0.01	1.10012±0.00038

4. RESULTS

Cross section data are shown in Figures 4 and 5 for carbon and beryllium respectively, comparing the experimental results to ENDF/B-VII.0 [5]. Carbon was chosen as an experimental standard due to the large volume of (previously) measured data as well as the consistency of the major cross section evaluations. Carbon also provides sharp resonance structure in the energy range of interest and this well-established structure can be used to assess the resolution of the current detection system. By showing good agreement between the carbon measurement and previous data the system and analysis method were validated. The beryllium were taken at the same time as the carbon data and analyzed with the same method.

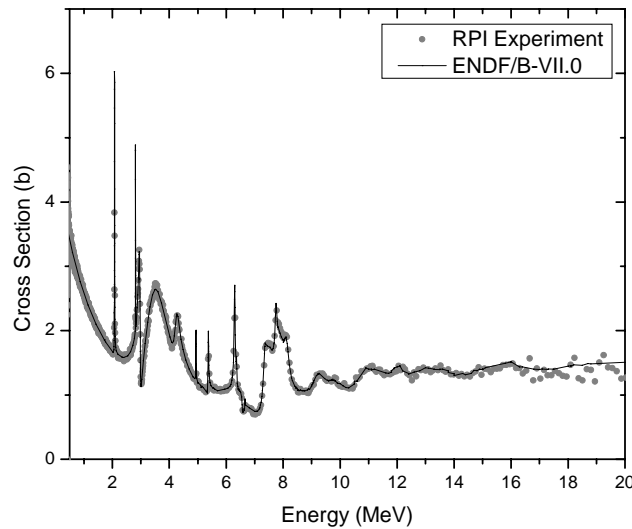


Figure 4: Carbon total cross section calculated from 13 cm sample with time of flight data grouped into 6.4 nsec channels

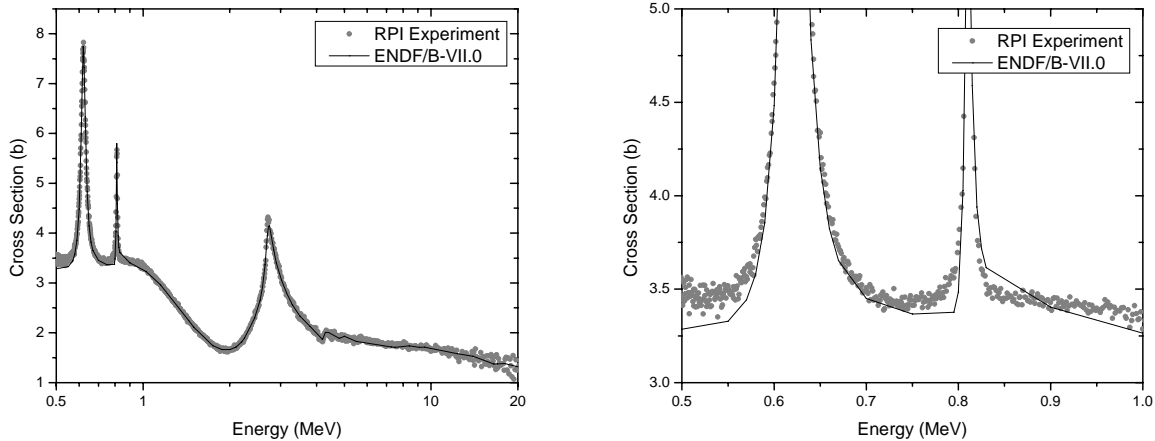


Figure 5: Beryllium total cross section calculated from combined samples with time of flight data grouped into 6.4 nsec channels (full range on left, zoomed view on right)

The carbon measurement shown is in agreement with ENDF/B-VII.0, illustrating that the measurement is highly accurate with good energy resolution in the range of 0.5 to 20 MeV. The beryllium measurement shows agreement above 1 MeV but displays some difference with ENDF/B-VII.0 in the range of 0.5 to 1 MeV. This difference of about 8% below 1 MeV confirms another measurement recently performed at the RPI Linac facility [6].

5. CONCLUSIONS

A new high energy time of flight system and background determination method has been discussed; and results for carbon and beryllium have been shown. The carbon results demonstrate the capability to accurately perform high quality transmission measurements in the energy range of 0.5 to 20 MeV at the RPI LINAC. The beryllium measurements provide new data to improve the experimental database. Below 1 MeV the ENDF/B-VII evaluation is about 8% lower than the experimental data which is consistent with the measurement discussed in reference [6].

REFERENCES

1. Eljen Technology. 2010 E. Broadway, Sweetwater TX 79556. URL: www.eljentechnology.com.
2. X-5 Monte Carlo Team, Computer code MCNP—A General Monte Carlo *N*-Particle Transport Code, Version 5, LA-UR-03-1987, April 24, 2003.
3. M. E. Overberg, B. E. Moretti, R. E. Slovacek and R. C. Block, “Photoneutron Target Development for the RPI Linear Accelerator”, *Nucl. Instrum. Meth. Phys. Res. A*, Vol. 253, pp. 438, 1999.

4. Y. Danon and R. C. Block, "Minimizing The Statistical Error of Resonance Parameters and Cross Sections Derived from Transmission Measurements", *Nuclear Instruments and Methods A*, Vol. 485, pp. 585-595, June 2002.
5. M.B. Chadwick, P. Oblozinsky, M. Herman et al., "ENDF/B-VII.0: Next Generation Evaluated Nuclear Data Library for Nuclear Science and Technology", *Nuclear Data Sheets*, Vol. 107, pp. 2931-3060, 2006.
6. Y. Danon, R. C. Block, M. J. Rapp, and F. J. Saglime, G. Leinweber, D. P. Barry, N. J. Drindak and J. G. Hoole, "Beryllium and Graphite High Accuracy Total Cross-Section Measurements in the Energy Range from 24 keV to 900 keV", *Nuclear Science and Engineering*, Vol. 162, March 2009.